[CANCER RESEARCH 62, 6263–6269, November 1, 2002]

Clustered DNA Damage Leads to Complex Genetic Changes in Irradiated Human Cells[1]

Belinda K. Singleton,[2] Carol S. Griffin, and John Thacker[3]

Medical Research Council, Radiation & Genome Stability Unit, Harwell, Oxfordshire OX11 0RD, England

ABSTRACT

Densely ionizing radiations interact with DNA to cause heavily clustered sites of damage that are difficult to repair correctly. We have been able to determine for the first time the breakpoints of several very large deletions induced by densely ionizing radiation in diploid human cells and show that damage clustering is reflected in the complexity of mutations. Intra- and interchromosomal insertions and inversions occur at the sites of some large deletions. Short sequence repeats are commonly found at the breakpoints, showing that microhomologies help patch damage sites. We suggest that novel fragments found in complex rearrangements derive from other sites of radiation damage in the same cell. These transmissible molecular changes are echoed by visible chromosome rearrangements many days after irradiation and are likely to contribute significantly to the carcinogenic properties of densely ionizing radiations.

INTRODUCTION

The accumulation of mutations that permit unrestrained growth of somatic cells may lead to cancer (1). In human cancer cells, mutations that activate proto-oncogenes or inactivate tumor suppressors are frequently the result of major chromosomal alterations, such as translocations, inversions, large deletions, and partial or complete loss of chromosomes, generically termed gross chromosomal rearrangements (2, 3). These rearrangements may form at many different sites in the large genome of mammalian cells, particularly after damage by carcinogens, and have therefore been difficult to analyze at the molecular level.

Carcinogens vary in the types of damage they cause to DNA. It is now considered that approximately half of the effective dose to humans from ionizing radiations comes from radon gas, a natural decay product of uranium present in the earth's surface. ^{222}Rn decays with a half-life of 3.8 days, emitting 5.5 MeV α-particles that produce densely ionizing radiation tracks when traversing biological material. For example, a single α-particle track has ~10,000 ionizations (equivalent to a dose of 150 mGy) when traversing a 12-μm human cell nucleus, whereas a γ-ray track has only ~30 ionizations (dose, 0.4 mGy) in the same nucleus (4). Therefore, there is no such thing as a low dose of α-particles to the cell. Because of the density of ionization, α-particle interaction with DNA will cause heavily clustered sites of damage (5, 6), consisting of a mixture of closely spaced base damage and breaks in the sugar-phosphate backbone. Although it is calculated that domestic exposure to radon gas contributes significantly to cancer incidence (7, 8), little is known about the molecular consequences of such clustered DNA damage.

In particular, we wished to ask whether the clustering of DNA damage after irradiation has its counterpart in mutational response, *i.e.,* complex molecular losses and rearrangements. This is not a trivial task, as noted above, because the possibility of loss or rearrangement of sequence over large genetic regions makes sequence-level analysis difficult, particularly in primary human material. We have used normal diploid human cells to study mutations caused by α-particles from a well-characterized source of ^{238}Pu, which emits α-particles of initial energy (5.5 MeV) similar to that of radon. Early-passage human cells should respond in ways that most closely reflect the cells of the intact organism, and they are chromosomally stable. However, such cells have a limited life span, which can make it difficult to analyze fully the molecular changes in mutants. We have chosen the X-linked *HPRT* gene as the target for mutation induction because mutant selection methods are well established and it is relatively tolerant to large genetic changes (see, for example, Ref. 9). Additionally, coherent genomic sequence data are available for *HPRT* (10) and for some of the surrounding region of Xq26, facilitating mapping of large mutational changes.

MATERIALS AND METHODS

Primary Cell Culture. HF12 primary male human fibroblast cells (11) at passage 3 were grown in Eagle's minimum essential medium (Life Technologies), with 2 mM L-glutamine, antibiotics, and 10% FCS. Cells from passages 3–8, having a normal cytogenetic profile, were used in mutant selection experiments. Growth to determine cloning efficiencies and surviving fractions was optimized using feeder layers irradiated with 30-Gy X-rays and respread at 1000 cells/cm^2. The average cloning efficiency was 49.7 $\pm$ 13.3%.

Preirradiation Growth and Irradiation Conditions. To reduce the frequency of spontaneous mutants present, cell stocks were grown from low cell numbers (1000–5000 cells) to ~10^7 cells. Stocks were seeded onto specially constructed 30-mm dishes with very thin (2.5 μm) plastic bases (12). Cells were irradiated through the dish bases at 3×10^5 cells/dish with ^{238}Pu α-particles (range, ~20 μm; peak energy, 3.26 MeV; linear energy transfer at the position of the cells, 121.4 keV/μm; Ref. 13). After irradiation, trypsinized cells from three dishes were pooled as a separately irradiated culture. In each experiment, 12–20 irradiated cultures were set up to isolate independently derived mutants. The immediate cell surviving fraction was determined by seeding 750 irradiated cells or 150 unirradiated cells into dishes with feeder cells and incubating these for 2 weeks to form colonies. In an initial experiment, cultures irradiated at either 25 or 50 cGy were pooled to determine mutant yield (mutants α1/25-1 and α1/50-4 came from this experiment). After this, independent mutants induced by 50 cGy were selected from 10 additional experiments. Spontaneous mutants were treated similarly but not irradiated.

Mutant Selection. Irradiated cells were grown nonselectively for a 7-day expression time and were then respread in dishes at 1000/cm^2 in 5 μg/ml 6-thioguanine for mutant selection (14) or at 150 per 9-cm dish without selection for cloning efficiency. Mutant frequency is expressed as the number of mutant clones detected divided by the number of cells seeded, corrected for cloning efficiency. Clones arising after 21–28 days in 6-thioguanine medium were isolated using micropipette tips. Picking one mutant per culture ensures independence, but sometimes more than one mutant was picked to offset losses attributable to senescence (in this case a mutant was considered as independently derived if it was found to have a molecular change in *HPRT* that was clearly different from those in mutants derived from the same culture). Otherwise, mutants were isolated randomly, without regard to colony size.

Molecular Analysis of Mutants. DNA was prepared from mass cell cultures or direct from cell colonies (15). PCR primer pairs were designed to cover the entire *HPRT* gene at ~1-kb intervals (14); after breakpoints were localized, additional primers were designed to isolate and sequence the mutant

Received 7/22/02; accepted 8/23/02.

The costs of publication of this article were defrayed in part by the payment of page charges. This article must therefore be hereby marked *advertisement* in accordance with 18 U.S.C. Section 1734 solely to indicate this fact.

[1] B. K. S. acknowledges a studentship from the Medical Research Council. This work was supported in part by European Communities Contract F13P-CT92-0007.

[2] Present address: Bristol Institute for Transfusion Sciences, Southmead Road, Bristol BS10 5ND, United Kingdom.

[3] To whom requests for reprints should be addressed, at MRC Radiation & Genome Stability Unit, Harwell, Oxfordshire OX11 0RD, England. Phone: (44) 1235-834393; Fax: (44) 1235-834776; E-mail: j.thacker@har.mrc.ac.uk.

junctions (not shown). The number of sites tested depended on the nature of the mutation; at least five sites were tested within the gene for each mutant. PCRs were duplicated and included an "outside marker" primer pair to detect genes on the short arm of the X-chromosome (either *DMD* or *STS*) to ensure that negative results were not attributable to failed reactions. The absence of PCR products indicated a genetic deletion, and all such reactions were repeated.

RAGE-PCR[4] (16) was used to amplify unknown regions of genomic DNA associated with *HPRT* mutations. This method involved the separate digestion of plasmid (pUC18) and human genomic DNA with restriction enzyme, followed by mixing in equal quantities and ligation of the fragments to each other (at 50 μg/ml in 10 μl). Several different restriction enzymes were used to attempt to get products of a size that could be PCR-amplified using nested primers designed to both the plasmid and genomic DNA sequences; this reaction usually gave no visible products in the first set of cycles, but could yield products in the second or third nested sets for at least one restriction enzyme. PCR products were sequenced directly.

Deletion breakpoints were searched for sequence features such as repeats, palindromes, and topoisomerase recognition sites, as described previously (9). Human genomic databases were searched for alignments to unknown sequences at breakpoints by use of BLASTN (17). PCR primers were designed to screen a human monochromosomal library (United Kingdom Human Genome Resource Centre), to analyze the origin of the L1 repeat sequence of mutant α4/3-1, by maximizing the difference at their 3′ ends between this L1 repeat and others in the genomic sequence databases.

Markers Linked to *HPRT*. Primers were as described previously (14, 18). Sequence data for DXS53 and DXS177 and the plasmid carrying DXS311 were kindly supplied by Dr. J. A. Nicklas (University of Vermont, Burlington). The DXS311 fragment was isolated and sequenced by standard methods to allow primer design. DXS144 was used in Southern analysis as a 1-kb *Pst*I fragment of the probe C11, supplied by Dr. J-L Mandel (CNRS, Strasbourg, France). The molecular distances and orientations cited in the text for these and other X-linked sequences were taken from data given in acedbX[5] and Lippert *et al.* (19).

Cytogenetic Analysis. HF12 cells were exposed to α-particle irradiation as described above. Cells were exposed to colcemid (0.1 μg/ml for 4 h) and harvested at 3 and 15 days after irradiation. Chromosomes 1, 2, and 5 were painted with FITC-labeled chromosome-specific probes (Cambio) as described previously (20). To analyze chromosomal changes in α-particle-induced mutants, the chromosomes were initially painted with biotin-labeled total X-chromosome probe (Cambio). Subsequently, M-FISH 24-color chromosome-specific paints were used as described (SpectraVysion assay protocol; Vysis). Pretreatment consisted of RNase A (100 μg/ml) for 1 h at 37°C and pepsin (50 μg/ml in 10 mM HCl) for 2 min at 20°C.

RESULTS

Many α-Particle-induced Mutations Are Large Deletions. HF12 cells grown on ultrathin plastic surfaces were irradiated with α-particles, and independently arising *HPRT* gene mutants were detected by their resistance to 6-thioguanine. An ~7-fold increase in mutant frequency was found, compared with unirradiated cells (Table 1). Mutant clones varied widely in their growth capacity; clonal expansion after selection was sufficiently poor in approximately one-fourth of the mutants to preclude analysis of the *HPRT* gene mutation.

More than 100 induced mutants (representing a minimum of 64 independently induced mutants) were classified by the presence/absence of PCR products for sites over the 60-kb *HPRT* genomic region. Approximately half of these mutants had large genetic changes, detectable as losses of part or all of the *HPRT* gene (Table 1). The remainder were classified as point mutations because all sites tested gave the correct-sized PCR product. On the basis of the same criteria, all 11 spontaneous mutants (a minimum of 8 independent mutants) had point mutations.

Table 1 *Survival and mutation of HF12 cells after α-particle irradiation*

Dose	Surviving fraction[a]	Mutant frequency[b]	No. (%) of large genetic changes[c]
None	(1)	$4.5 \pm 1.2 \times 10^{-6}$	0/11 (0)
0.5 Gy	0.25 ± 0.05	$30.6 \pm 5.5 \times 10^{-6}$	35/64 (55)

[a] Measured by respreading cells immediately after irradiation (mean of eight experiments ± SE).

[b] Measured after a 7-day expression time (for α-particles, from a mean of 10 experiments ± SE). The increased frequency after α-particle irradiation is highly significant ($P = 0.0003$).

[c] PCR-based assessment, where large changes include >100-bp alterations in product size for multiple sites across the *HPRT* gene (see Fig. 1).

It was possible to determine with some certainty the localization of the deletion breakpoints for a subset of the α-particle-induced mutants. First, approximately half of the deletions were found to have at least one breakpoint within the *HPRT* gene (Fig. 1, *upper part*). Second, where deletion breakpoints extended either proximally or distally into "unknown" sequences adjacent to *HPRT*, it was found that deletion breakpoints were distributed throughout the Xq26 region (Fig. 1, *lower part*). The deletion in one mutant, α9/9-1, extended beyond the most proximal and distal markers tested to give a deletion size of at least 3 Mb. Third, the chromosomes of mutants with partial or total *HPRT* deletions were examined with a total X-chromosome probe. None of the deletion mutants examined showed an X-chromosome rearrangement except for mutant α11/10-1, which showed a translocation located at approximately Xq26. Further analysis by M-FISH, in which each chromosome is colored differently, identified the translocation in mutant α11/10-1 as an X:9 reciprocal translocation and showed that this mutant had further translocations (Fig. 2*A*). M-FISH was used to look at other mutants with large *HPRT* deletions, and in each case other gross chromosomal rearrangements, not involving the X-chromosome, were identified (data not shown).

Rejoining at Microhomologies Characterizes Large Deletion Junctions. Deletion mutants that had one or both breakpoints within the *HPRT* gene were chosen for detailed analysis. Where deletions extended into unknown sequences, we used RAGE-PCR on DNA from both mutant and wild-type cells (see "Materials and Methods") to define the sequence on both sides of a breakpoint. In the following descriptions, the term "breakpoint" is used to indicate the position at which the break occurred in nonmutant DNA, whereas the term "junction" indicates the rejoined mutant sequence (*i.e.*, there are two breakpoints and one junction in simple deletion mutants).

Mutant α1/50-4 had a simple internal *HPRT* deletion of 505 bp, including exon 4 (Fig. 1). A 2-bp (CT) direct repeat was present at the breakpoints (Fig. 3), and there was a strong consensus recognition site for DNA topoisomerase II (21) overlapping the upstream breakpoint (Fig. 3, *vertical arrow*). Mutant α1/25-1 had a deletion extending into unknown sequence upstream of *HPRT* (Fig. 1), but use of RAGE-PCR to identify the sequence in wild-type DNA showed again that a 2-bp (TG) repeat occurred at the breakpoints (Fig. 3). The downstream breakpoint (in the *HPRT* gene) was in an *Alu* repeat, but no corresponding repeat sequence occurred at the upstream breakpoint. Searches for the unknown sequence identified a 100-kb BAC clone (bWDX180) that overlapped with another fully sequenced BAC (bWDX187) carrying the *HPRT* gene; alignment of these two BAC sequences showed that a deletion of 75,164 bp had occurred in mutant α1/25-1.

Complex Genetic Rearrangements at Large Deletion Junctions. Mutant α8/3-1 had a still larger deletion, shown by loss of DXS79 but retention of 299R (~700 kb upstream; Fig. 1). Sequence of the mutant junction, followed by identification and sequencing of the breakpoints in wild-type DNA by use of RAGE-PCR showed that 3 bp of additional sequence (TTC) occurred at the mutant junction (Fig. 3). The upstream breakpoint occurred in an *Alu* repeat, but no repeat was

[4] The abbreviations used are: RAGE, rapid amplification of genomic ends; L1, LINE-1; M-FISH, multiplex fluorescence *in situ* hybridization; BAC, bacterial artificial chromosome; PAC, P1 artificial chromosome; DSB, double-strand break.

[5] http://webace.sanger.ac.uk.

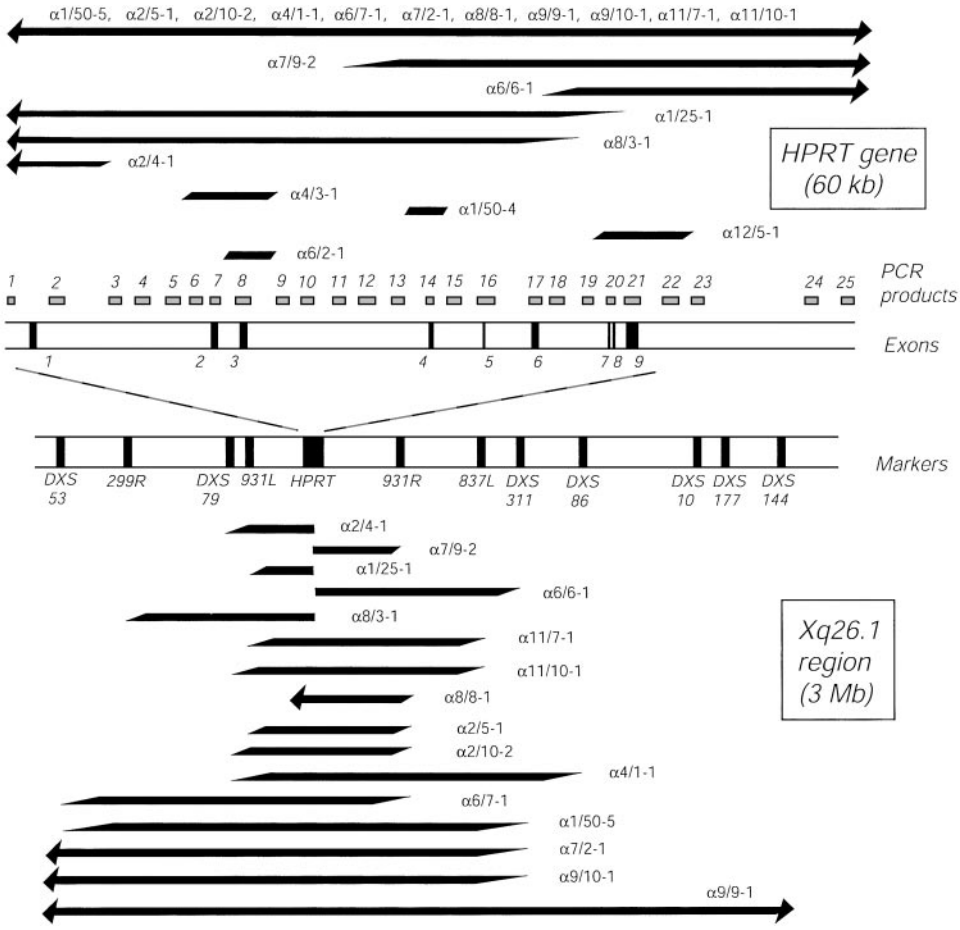

Fig. 1. Breakpoint distribution of α-particle-induced mutants. *Upper diagram*, *HPRT* gene showing intron/exon structure and sites of PCR products used to assess the presence/absence of different parts of the gene. *Lower diagram*, Xq26.1 genomic region, showing the sites of flanking markers (*black bars*). The positions of deletions in specific mutants are shown as *filled rectangles*, with *sloping ends* indicating the uncertainties of position; *arrows* indicate that the deletion goes beyond that point. Mutants with deletions that go beyond the end(s) of *HPRT* are shown in both the upper and lower diagrams.

found at the downstream breakpoint. Searches of human genomic sequence databases found an exact match for the unknown sequence to a partially sequenced BAC clone (RP11-274K13). This clone mapped to the X-chromosome but was at least 1 Mb downstream of *HPRT* (Fig. 4*A*), indicating that the relative positions of the remaining *HPRT* sequence and the unknown sequence were inverted in the mutant sequence.

Two other mutants, α12/5-1 and α4/3-1, were initially considered to be simple internal *HPRT* deletions, each of ~4 kb (Fig. 1), but PCR primers designed to amplify the *HPRT* sequence on either side of the mutant junction failed to give products. Use of RAGE-PCR revealed that the *HPRT* mutant breakpoints were now joined to unknown sequence on each side (giving at least four breakpoints and two junctions in each mutant). The simplest explanation for this finding was that unknown sequence had been inserted at the deletion site in *HPRT*.

Sequencing across the proximal junction of the α12/5-1 mutant gave unknown sequence, which was found to map to the X-chromosome at a position 3.4 Mb upstream of *HPRT* (defined by the PAC clone RP1-37M17; Fig. 4*A*, *upper part*). The sequence TTTCC immediately adjacent to the proximal junction has been found previously at some radiation-induced mutant junctions (14, 22), and again the *HPRT* breakpoint occurred in an *Alu* repeat (Fig. 3). The *HPRT* breakpoint at the distal junction occurred in a Donehower repeat and had a 2-bp (CA) direct repeat with the unknown sequence. The unknown downstream breakpoint was within a L1 repeat, which has been mapped to Xq25–26.2.

The complexity of mutant junctions was even greater in the final mutant analyzed, α4/3-1. The unknown breakpoints at both proximal and distal junctions were linked to an X-chromosome sequence usually found 2.9 Mb upstream (defined by another recently sequenced PAC clone, RP1-119E23; Fig. 4*A*, *upper part*). However, one of these upstream sequences was present in the mutant in the opposite orientation with respect to *HPRT*, indicating that a sequence inversion had occurred at this junction. To add to the complexity, the proximal junction had an insertion of unknown sequence between the RP1-119E23 sequence and *HPRT*. Searches revealed an exact match for the unknown sequence to part of a L1 repeat from a partially sequenced BAC clone (RP11-172E10) mapped to chromosome 8. Because spurious clone assignments can occur, the location of this sequence in nonmutant cells was confirmed by screening a monochromosomal library using PCR primers designed to detect uniquely the inserted sequence (Fig. 4*B*). The proximal *HPRT* breakpoint was part of an *Alu* repeat, and unusually, a 7-bp sequence common to *HPRT* and the unknown sequence was present close to the junction (Fig. 3). At the distal breakpoints, 4-bp direct repeats (CATA) occurred, and these repeats were themselves within other short repeats (*e.g.*, ATA/CATAC at the *HPRT* breakpoint).

Similar Genetic Changes Are Detected by Molecular and Microscopic Analysis. Are the α-particle-induced mutations in the *HPRT* gene, which are mostly not visible with the light microscope, part of a spectrum of transmissible large genetic changes including those seen microscopically? The translocation in mutant α11/10-1 supports this idea, but to answer this question directly is technically difficult because it would require the molecular detection and sequencing of randomly induced sites of visible radiation-induced changes. To strengthen this association, we used FISH to

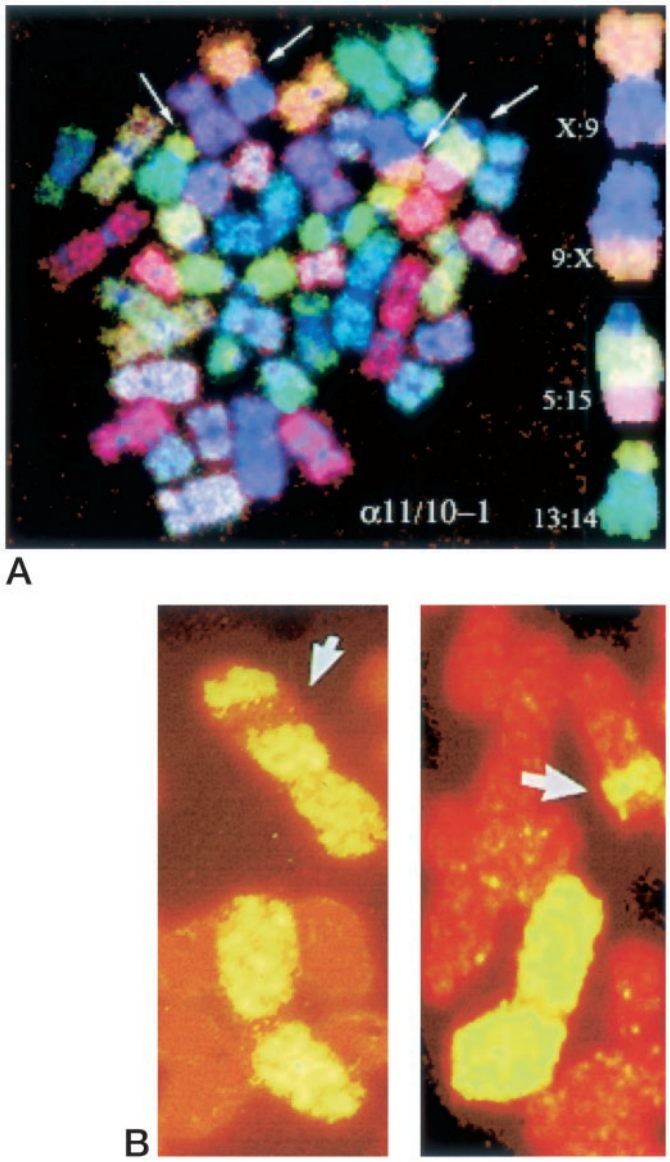

Fig. 2. FISH chromosomal analysis of a large deletion mutant and irradiated HF12 cells. *A*, M-FISH analysis of mutant α11/10-1, showing reciprocal X:9 translocation and nonreciprocal 5:15 and 13:14 translocations. Rearranged chromosomes are indicated by *arrows* and are shown enlarged at the *right*. *B*, examples of large insertions (*arrows*) into nonhomologous chromosomes of unselected cells found at 15 days after α-particle irradiation.

determine whether similar types of visible genetic change (deletion, insertion, inversion) could be found in the chromosomes of large numbers of irradiated HF12 cells without selection for mutation. As seen in Table 2, at 3 days after irradiation, when most cells had recovered from radiation-induced division delay, a high frequency of unstable chromosomal changes (*e.g.*, dicentrics and fragments) were present, but with time in culture their frequency declined sharply. Potentially stable changes, such as translocations, persisted at approximately the same frequency over 15 days of culture, and the occasional inversion was detectable at both 3 and 15 days after irradiation. Complex rearrangements, which by definition include insertions (Table 2), declined by half at 15 days because of the loss of unstable types. Significantly, given our molecular data, at 15 days almost all of these rearrangements were stable interchromosomal insertions of fragments, as depicted in Fig. 2*B*.

MUTANT α1/50-4

```
(HPRT) (27679)                    ⇓
upstream    ACTTTTTAATTTTTACTAATCT CT ACTTGAAAGTTTTCTAGTCATTC
            ||||||||||||||||||||||| ||   ||  | | |  |      ||
junction    ACTTTTTAATTTTTACTAATCT CT CTGTGGGACTCTAATTTGGGATC
            | | |  | |  |      |   || ||||||||||||||||||||||
downstream ATTGTCAAGTACTGCTGTCTGC CT CTGTGGGACTCTAATTTGGGATC
(HPRT)                            (28186)
```

MUTANT α1/25-1

```
(unknown)
upstream    TTCATTATATCATTTTTACATGA TG TGCTATCAGGTAACCAAAATTC
            ||||||||||||||||||||||| ||  |  |    | ||       ||
junction    TTCATTATATCATTTTTACATGA TG GGTGACAGAGCAAGACTCCGTC
               |    |    | ||      || ||||||||||||||||||||||
downstream GATCGTGCCACTGCACTCCAGTC TG GGTGACAGAGCAAGACTCCGTC
(HPRT)                           (41203)
            ||||| ||||||||||||||| | || || |||||||| ||||||||||
Alu.con     GATCGCGCCACTGCACTCCAGCC TG GGCGACAGAGCGAGACTCCGTC
```

MUTANT α8/3-1

```
Alu.con     CTGTAATCCCAGCACTTTGGGA    GGCCGAGGTGGGTGGATCACCT
            || ||||||||||||||||||    ||||| || ||||||||||
(unknown)
upstream    CTATAATCCCAGCACTTTGGGA    GGCCGTGGCGGGTGGATCACGA
            ||||||||||||||||||||||      | ||    ||  |  |
junction    CTATAATCCCAGCACTTTGGGAttcAATCTTGTAATGTCTAATATTT
               | |     | |   |   |    ||||||||||||||||||||||
downstream GATTGAGTTTTGGAGGGTCACA    AATCTTGTAATGTCTAATATTT
(HPRT)                      (36475)
```

MUTANT α12/5-1 (proximal junction)

```
Alu.con      ACTAAAAATACAAAAA--TTAGC CGGGCGTGGTGGCGCGCGCC
             |||||| | | |||||  ||||| |||| ||| ||||| | |||
(HPRT)                        (39228)
upstream     ACTAAATACAAAAAAAAATTAGC CGGGAGTGCTGGCGGGGTGCC
             |||||||||||||||||||||||         ||      ||
junction     ACTAAATACAAAAAAAAATTAGC TTTCCTGCCTTCTTCATGTT
                |                    |      ||||||||||||||||||||
downstream   TTTCTCCTGGCTCTGGATCACAT TTTCCTGCCTTCTTCATGTT
(unknown)
```

MUTANT α12/5-1 (distal junction)

```
(unknown)
upstream    ATCCCATTATTAAAAAGTCAGAA CA CAATAGATGTTGGCATGGATA
            |||||||||||||||||||||||| ||   ||        |   ||
junction    ATCCCATTATTAAAAAGTCAGAA CA GGATCACACAGCTAGTAAGTA
                  | | | | |   || ||||||||||||||||||||||
downstream CCAGAGAGGTCACATAATTTGCC CA GGATCACACAGCTAGTAAGTA
(HPRT)                    (44098)
            ||||||||| |  ||| ||||| ||  | ||||||||||
Don.con     ACAGAGAGGTTAAGTANCTTGCC CA AGGTCNCNNANCN
```

MUTANT α4/3-1 (proximal junction)

```
Alu.con     AGGTCAGGAGTTCAAGACCAG CCTGGCCAACATGGTGAAACC
            |   |||||||||||||||||| ||||| |||||| | || ||
(HPRT)                           (12240)
upstream    ATCCCAGGAGTTCAAGACCAG CCTGGGCAACATAGCGAGACT
            ||||||||||||||||||||||         |   |     |
junction    ATCCCAGGAGTTCAAGACCAG TAGAAGACAATGTGTTGATCC
               |  |||||||      | ||||||||||||||||||||||
downstream GGTAAATTAGTTCAACCATTG TAGAAGACAATGTGTTGATCC
(unknown)
```

MUTANT α4/3-1 (distal junction)

```
(unknown)
upstream    ACACACACATATTTGTACACT CATA TACACATATATAATATCCCT
            |||||||||||||||||||||| ||||                |   |
junction    ACACACACATATTTGTACACT CATA CTGGTGACAGATACCCTCTC
               | || | |||    |   |||| ||||||||||||||||||||||
downstream  TGGGATACTTTTTTCACTATA CATA CTGGTGACAGATACCCTCTC
(HPRT)                           (17060)
```

Fig. 3. Sequences of breakpoints in selected deletion mutants. For each mutant, ~50 bp of the upper strands (5′→3′) are shown for the intact upstream (*top*) and downstream (*bottom*) sequence, with the mutant sequence in the middle (junction). Where sequences have homology to *Alu* or Donehower repeats, this is illustrated by the consensus (*.con*) sequence. *Vertical bars* between bases indicate homology; where a direct repeat occurs at the breakpoints, there is a *space* on either side of the repeat. The position of the breakpoint in the genomic *HPRT* sequence (10) is indicated by the base number (in *parentheses*). Sequence features include potential topoisomerase II sites (predicted cutting site indicated by *vertical arrow*), direct/inverted repeats (*bold*), near matches to the short deletion consensus (*underlined*), the recombination hot-spot *Chi* sequence (*bold underlined*), the 3′ core ARS sequence (*italics*), the heptamer/nonamer signal sequence (*bold italics*), and a radiation mutant sequence (*italic underlined*). Inserted nucleotides are shown in *lowercase* (mutant α8/3-1). The *gray-shaded* sequences in mutant α4/3-1 are inverted repeats in the proximal and distal *HPRT* breakpoint sequences (see Fig. 5).

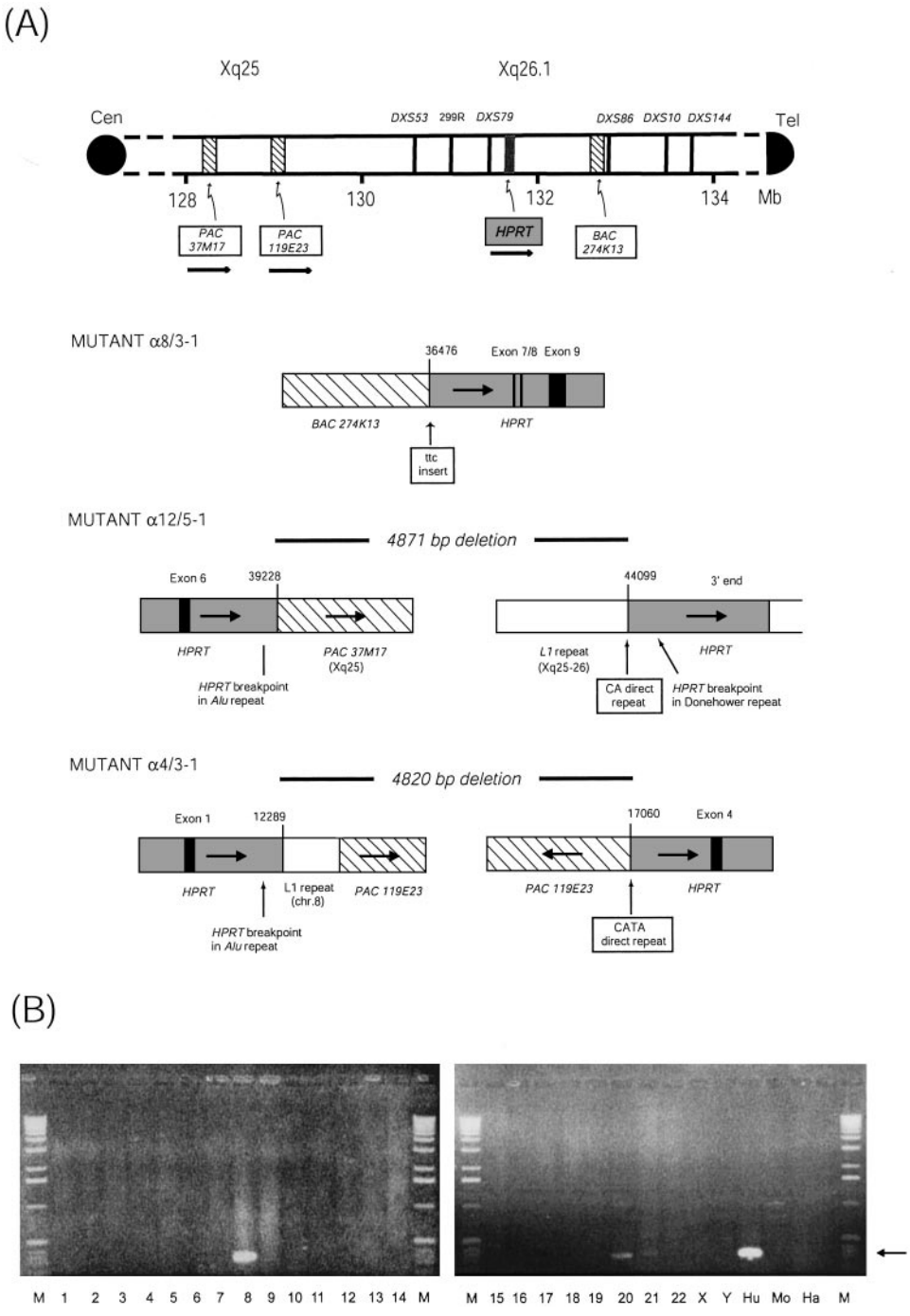

Fig. 4. Molecular rearrangements in complex deletion mutants. *A, upper part*, the genomic organization of chromosome Xq25–26, with sequences found to be rearranged with *HPRT* indicated in *boxes* (see text). *Arrows* indicate orientation, where known, relative to the centromere (*Cen*) and telomere (*Tel*). *Lower part*, structure of complex mutant junctions. *Numbering* above mutant junctions is the position of the breakpoint in *HPRT* genomic sequence. *B*, PCR screen of a monochromosomal library for the presence of the inserted proximal junction sequence in mutant α4/3-1 showing its origin in chromosome 8 (with a slight cross-reaction to chromosome 20). *Lane M*, 1-kb ladder (Life Technologies); *Lanes 1–22*, individual human chromosomes; *Lane Hu*, human genomic DNA; *Lane Mo*, mouse genomic DNA; *Lane Ha*, hamster genomic DNA.

DISCUSSION

We have shown that it is possible to carry out detailed molecular analysis of large and complex genetic changes induced by α-particles in the *HPRT* gene of human diploid fibroblasts, despite their limited life span. To complement these molecular data, we assessed genome-wide changes in the same irradiated primary cells by cytogenetic analysis to show that similar types of transmissible changes may be found, conceptually linking together molecular and visible genetic changes.

Mechanisms of Mutation in Primary Human Cells. Our success in sequencing both sides of each breakpoint in these mutants allows comment on mechanisms of deletion and rearrangement formation. At the radiation dose used (0.5 Gy), knowing the average projected nuclear area of the HF12 human cells in this experimental situation (mode, 225 μm^2; Ref. 20), approximately five α-particle tracks would occur in each nucleus traversed. These tracks will yield 30–40 DSBs/nucleus, but the DSBs will be distributed nonrandomly such that most will be part of a cluster of several ($\geq$4) DSBs within megabase intervals, with a few much larger clusters (23). Additionally, each DSB will be associated with base damage in these localized sites. Repair of base damage within a heavily clustered damage site is likely to occur relatively slowly and can lead to further DSBs, either through inopportune endonuclease action at base damage on complementary DNA strands or through interaction of base damage with the replication machinery (24).

The rejoining of DSBs can be accomplished by repair pathways,

Table 2 *Chromosomal aberrations induced by α-particles in HF12 cells (FISH analysis of chromosomes 1, 2, and 5)*

Days after irradiation	Cells scored	Aberration numbers (%)[a]					
		Dicentric	Fragment	Translocation	Ring	Inversion[b]	Complex[c] (incl. insertion)
Unirradiated							
All days[d]	446	0	2 (0.5)	1 (0.2)	0	0	0
Irradiated							
3 days	471	12 (2.5)	14 (3.0)	26 (5.5)	5 (1.1)	1 (0.2)	8 (1.7)
15 days	883	1 (0.1)	2 (0.2)	43 (4.9)	2 (0.2)	1 (0.1)	7 (0.8)

[a] Classified according to Savage and Simpson (50).
[b] Underestimated because intra-arm events are not scorable.
[c] Includes insertions as shown in Fig. 2*B*; at 3 days, complex aberrations consisted of four stable and four unstable types, whereas at 15 days there were six stable to one unstable. All of the stable complex aberrations were insertions.
[d] Pooled from scores taken over the period 3–15 days (individual days were not significantly different).

including homologous recombination and nonhomologous end joining (reviewed in Refs. 25, 26). Although it has been established in principle that interchromosomal homologous recombination can give rise to translocations in mammalian cells (27), breakpoint sequence analysis of the present series of mutants gave little indication that interaction of homologous sequences was involved. Lengthy repeat sequences such as *Alu* occurred only at one breakpoint in any mutant and were sufficiently common for these to have been associated with the mutation site by chance. Similarly, the occurrence of short sequence motifs, indicating the involvement of specific enzymatic processes in the induction and/or processing of damage, was not common at breakpoints (Fig. 3). A DNA topoisomerase II cleavage site at the upstream breakpoint of mutant α1/50-4 may be significant because topoisomerase II has previously been implicated in deletion formation (28), potentially through enhanced cleavage of DNA at sites of base damage (29, 30). Mutant α8/3-1 alone had a short (3 bp) sequence insertion at the deletion junction and occurred distally to *HPRT* exon 6. Interestingly, small deletions with breakpoints in exon 6 have been found with inserted bases that are inverted complements of sequences at the breakpoints (31); these deletions commonly have the triplet TTC at the breakpoint.

It is significant that all of the mutants except α8/3-1 had short sequence repeats (microhomologies) of 2–5 bp present at one pair of breakpoints and that one copy of the repeat was lost in the mutant. The presence of microhomologies at sites of DSB rejoining has been observed in some previous studies with mammalian and yeast cells (32, 33) and in human cell extracts (34). Short inverted repeats may be involved similarly at sites of rejoining, where single-stranded "hairpin" structures are formed, which can be resolved by loss or inversion of the looped-out DNA (35, 36). It is possible to model some of the more complex junctions in these mutants by use of microhomologies as rejoining sites; for example, in mutant α4/3-1, it is striking that inverted repeat sequences (ACCAG/CTGGT) occurred at the proximal and distal *HPRT* breakpoints (Fig. 3). Starting with the annealing of these inverted repeats in single-stranded DNA, the structure of the α4/3-1 junctions is modeled in Fig. 5. The DNA in the "internal" loop, including *HPRT* exons 2 and 3, was replaced by external sequences that annealed at the sites of microhomology at or close to their ends, and the structure could be resolved by rejoining at the junctions.

It is not clear why microhomologies are used in end joining, because it can take place without any homology (DNA-protein kinase-dependent nonhomologous end joining; Ref. 37). One possibility would be that certain damage sites are difficult to repair by nonhomologous end joining and may require the activity of other repair proteins. Repair difficulties might arise by virtue of damage location, such as proximity to noncanonical DNA structures (38), or, in the present case, because of clustering of damage.

Complexity of α-Particle-induced Mutations. In addition to intrachromosomal complexity, mutant α4/3-1 carried an insertion into *HPRT* of a fragment from a L1 element from chromosome 8, showing that interchromosomal interactions are stimulated. We have supported this finding by showing that visible interchromosomal insertions are not uncommon many days after α-particle irradiation (Fig. 2*B*; Table 2). Spontaneously occurring insertions are relatively rare events in the human genome; in the germ line these account for ~1 in 600 mutations and mostly derive from endonuclease-dependent L1 element transposition (39). However, at sites of DNA breakage, truncated L1 insertions can occur by endonuclease-independent transposition, and these are accompanied by deletions of the target site (40). Significantly, where L1 insertions have been found in association with tumorigenesis, they show internal rearrangements, including deletions and inversions (41, 42). Similarly, in mutant α4/3-1, a truncated L1 sequence was inserted into *HPRT* alongside another X-linked sequence (identified by PAC 119E23), part of which had become inverted relative to the normal sequence. We think that it is unlikely that both parts of the 119E23 sequence inserted separately into *HPRT*, suggesting that the α4/3-1 rearrangement had undergone further rearrangement.

Recent experiments with both yeast and mammalian cells show that "capture" of DNA sequence to patch DSBs can make use of any linear end to rejoin break sites and that these insertions are derived from the most abundant sources of available ends (43, 44). The rarity of these simple insertions suggests first that end joining normally gives relatively precise ligation of DSBs with few sequence rearrangements. Second, it suggests that the patching of breaks with endogenous DNA fragments is

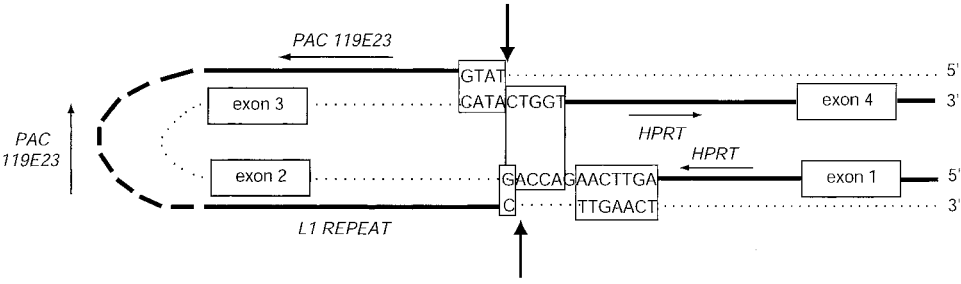

Fig. 5. Mechanism of formation of a complex mutant junction: proximal and distal *HPRT* junctions in mutant α4/3-1. Single-stranded DNA from the *HPRT* gene is shown *centrally*, held in a loop by annealing at a 5-bp inverted repeat (*boxed central sequence*; see also Fig. 3). DNA from other sources as indicated is rejoined at the *HPRT* breakpoints through annealing at direct repeats (*boxed*). *Vertical arrows* indicate the sites of breakage and rejoining. *Thick line* is conserved sequence; *dotted line* is deleted sequence.

limited by the availability of fragments. We suggest that when irradiation causes dense clusters of DNA damage, repair is inefficient (45) and many short DNA fragments are produced (46), providing more opportunity for patching to occur at damage sites. Therefore, an intriguing prediction of our analysis is that the captured fragments found in complex α-particle-induced mutants derive from collateral α-particle damage elsewhere in the genome. If this is true, then it may be possible to link rearrangements on different chromosomes and derive a molecular inventory of radiation-induced large genetic changes within a damaged cell.

Our data contrast strikingly with similar studies of large genetic rearrangements found after treatment with other DNA-breaking agents, such as bleomycin and neocarzinostatin. These chemically induced rearrangements were highly conservative, with almost no loss of sequence at the sites of DNA breakage (47–49). This comparison reinforces the conclusion that the heavy clustering of DNA damage from α-particle irradiation leads to the complex genetic changes we observed at the sequence level. Analysis at the visible (chromosomal) level will represent only the tip of the iceberg, considerably underestimating the extent and complexity of radiation-induced rearrangements. An important feature of these molecular changes is that they can be transmitted through mitotic divisions. At the sequence level, we see intra- and interchromosomal insertions and inversions in association with some large deletions, both indicators of genetic instability and potentially of carcinogenesis.

ACKNOWLEDGMENTS

We are grateful to Walter Masson, Paul Simpson, and Cathryn Tambini for help at various stages of these experiments and to David Stevens for the irradiations.

REFERENCES

1. Vogelstein, B., and Kinzler, K. W. The multistep nature of cancer. Trends Genet, *9:* 138–141, 1993.
2. Mitelman, F., Mertens, F., and Johansson, B. A breakpoint map of recurrent chromosomal rearrangements in human neoplasia. Nat. Genet., *15:* 417–474, 1997.
3. Lengauer, C., Kinzler, K. W., and Vogelstein, B. Genetic instabilities in human cancers. Nature (Lond.), *396:* 643–649, 1998.
4. Goodhead, D. T. Track structure considerations in low dose and low dose rate effects of ionizing radiation. Adv. Radiat. Biol., *16:* 7–44, 1992.
5. Goodhead, D. T. Initial events in the cellular effects of ionizing radiations: clustered damage in DNA. Int. J. Radiat. Biol., *65:* 7–17, 1994.
6. Ward, J. F. The complexity of DNA damage: relevance to biological consequences. Int. J. Radiat. Biol., *66:* 427–432, 1994.
7. Little, J. B. What are the risks of low-level exposure to alpha radiation from radon? Proc. Natl. Acad. Sci. USA, *94:* 5996–5997, 1997.
8. BEIR-VI. Health Effects of Exposure to Radon: BEIR VI. Washington DC: National Academy Press, 1998.
9. Morris, T., and Thacker, J. Formation of large deletions by illegitimate recombination in the HPRT gene of primary human fibroblasts. Proc. Natl. Acad. Sci. USA, *90:* 1392–1396, 1993.
10. Edwards, A., Voss, H., Rice, P., Civitello, A., Stegemann, J., Schwager, C., Zimmermann, J., Erfle, H., Caskey, C. T., and Ansorge, W. Automated DNA sequencing of the human HPRT locus. Genomics, *6:* 593–608, 1990.
11. Cox, R., and Masson, W. K. Changes in radiosensitivity during the in vitro growth of diploid human fibroblasts. Int. J. Radiat. Biol., *26:* 193–196, 1974.
12. Thacker, J., Stretch, A., and Goodhead, D. T. The mutagenicity of alpha particles from plutonium-238. Radiat. Res., *92:* 343–352, 1982.
13. Goodhead, D. T., Bance, D. A., Stretch, A., and Wilkinson, R. E. A versatile plutonium-238 irradiator for radiobiological studies with α-particles. Int. J. Radiat. Biol., *59:* 195–210, 1991.
14. Morris, T., Masson, W., Singleton, B., and Thacker, J. Analysis of large deletions in the HPRT gene of primary human fibroblasts using the polymerase chain reaction. Somat. Cell Mol. Genet., *19:* 9–19, 1993.
15. Aghamohammadi, S. Z., Morris, T., Stevens, D. L., and Thacker, J. Rapid screening for deletion mutations in the hprt gene using the polymerase chain reaction: X-ray and α-particle mutant spectra. Mutat. Res., *269:* 1–7, 1992.
16. Mizobuchi, M., and Frohman, L. A. Rapid amplification of genomic DNA ends. Biotechniques, *15:* 214–216, 1993.
17. Altschul, S. F., Gish, W., Miller, W., Myers, E. W., and Lipman, D. J. Basic local alignment search tool. J. Mol. Biol., *215:* 403–410, 1990.
18. Fuscoe, J. C., Nelsen, A. J., and Pilia, G. Detection of deletion mutations extending beyond the HPRT gene by multiplex PCR analysis. Somat. Cell Mol. Genet., *20:* 39–46, 1994.
19. Lippert, M. J., Albertini, R. J., and Nicklas, J. A. Physical mapping of the human *hprt* chromosomal region (Xq26). Mutat. Res., *326:* 39–49, 1995.
20. Griffin, C. S., Marsden, S. J., Stevens, D. L., Simpson, P., and Savage, J. R. Frequencies of complex chromosome exchange aberrations induced by ^{238}Pu α-particles and detected by fluorescence in situ hybridization using single chromosome-specific probes. Int. J. Radiat. Biol., *67:* 431–439, 1995.
21. Spitzner, J. R., and Muller, M. T. Application of a degenerate consensus sequence to quantify recognition sites by vertebrate DNA topoisomerase II. J. Mol. Recognit., *2:* 63–74, 1989.
22. Forrester, H. B., Radford, I. R., and Dewey, W. C. Selection and sequencing of interchromosomal rearrangements from gamma-irradiated normal human fibroblasts. Int. J. Radiat. Biol., *75:* 543–551, 1999.
23. Sachs, R. K., Brenner, D. J., Hahnfeldt, P. J., and Hlatkys, L. R. A formalism for analysing large-scale clustering of radiation-induced breaks along chromosomes. Int. J. Radiat. Biol., *74:* 185–206, 1998.
24. Dianov, G. L., O'Neill, P., and Goodhead, D. T. Securing genome stability by orchestrating DNA repair: removal of radiation-induced clustered lesions in DNA. Bioessays, *23:* 745–749, 2001.
25. Haber, J. E. Partners and pathways repairing a double-strand break. Trends Genet., *16:* 259–264, 2000.
26. Kanaar, R., Hoeijmakers, J. H., and van Gent, D. C. Molecular mechanisms of DNA double strand break repair. Trends Cell Biol., *8:* 483–489, 1998.
27. Richardson, C., and Jasin, M. Frequent chromosomal translocations induced by DNA double-strand breaks. Nature (Lond.), *405:* 697–700, 2000.
28. Bae, Y. S., Kawasaki, I., Ikeda, H., and Liu, L. F. Illegitimate recombination mediated by calf thymus DNA topoisomerase II *in vitro*. Proc. Natl. Acad. Sci. USA, *85:* 2076–2080, 1988.
29. Li, T. K., Chen, A. Y., Yu, C., Mao, Y., Wang, H., and Liu, L. F. Activation of topoisomerase II-mediated excision of chromosomal DNA loops during oxidative stress. Genes Dev., *13:* 1553–1560, 1999.
30. Sabourin, M., and Osheroff, N. Sensitivity of human type II topoisomerases to DNA damage: stimulation of enzyme-mediated DNA cleavage by abasic, oxidized and alkylated lesions. Nucleic Acids Res., *28:* 1947–1954, 2000.
31. Rainville, I. R., Albertini, R. J., and Nicklas, J. A. Breakpoints and junctional regions of intragenic deletions in the HPRT gene in human T-cells. Somat. Cell Mol. Genet., *21:* 309–326, 1995.
32. Roth, D. B., and Wilson, J. H. Nonhomologous recombination in mammalian cells: role for short sequence homologies in the joining reaction. Mol. Cell. Biol., *6:* 4295–4304, 1986.
33. Kramer, K. M., Brock, J. A., Bloom, K., Moore, J. K., and Haber, J. E. Two different types of double-strand breaks in Saccharomyces cerevisiae are repaired by similar RAD52-independent, nonhomologous recombination events. Mol. Cell. Biol., *14:* 1293–1301, 1994.
34. Thacker, J., Chalk, J., Ganesh, A., and North, P. A mechanism for deletion formation in DNA by human cell extracts: the involvement of short sequence repeats. Nucleic Acids Res., *20:* 6183–6188, 1992.
35. Sommer, S. S., and Ketterling, R. P. A postulated mechanism for deletions with inversions. Am. J. Hum. Genet., *52:* 1016–1018, 1993.
36. Gordon, A. J. E., and Halliday, J. A. Inversions with deletions and duplications. Genetics, *140:* 411–414, 1995.
37. Jeggo, P. A. DNA breakage and repair. Adv. Genet., *38:* 185–218, 1998.
38. Gordenin, D. A., and Resnick, M. A. Yeast ARMs (DNA at-risk motifs) can reveal sources of genome instability. Mutat. Res., *400:* 45–58, 1998.
39. Kazazian, H. H. An estimated frequency of endogenous insertional mutations in humans. Nat. Genet., *22:* 130, 1999.
40. Morrish, T. A., Gilbert, N., Myers, J. S., Vincent, B. J., Stamato, T. D., Taccioli, G. E., Batzer, M. A., and Moran, J. V. DNA repair mediated by endonuclease-independent LINE-1 retrotransposition. Nat. Genet., *31:* 159–165, 2002.
41. Miki, Y., Nishisho, I., Horii, A., Miyoshi, Y., Utsunomiya, J., Kinzler, K. W., Vogelstein, B., and Nakamura, Y. Disruption of the APC gene by a retrotransposal insertion of L1 sequence in a colon cancer. Cancer Res., *52:* 643–645, 1992.
42. Morse, B., Rotherg, P. G., South, V. J., Spandorfer, J. M., and Astrin, S. M. Insertional mutagenesis of the myc locus by a LINE-1 sequence in a human breast carcinoma. Nature (Lond.), *333:* 87–90, 1988.
43. Yu, X., and Gabriel, A. Patching broken chromosomes with extranuclear cellular DNA. Mol. Cell, *4:* 873–881, 1999.
44. Lin, Y., and Waldman, A. S. Promiscuous patching of broken chromosomes in mammalian cells with extrachromosomal DNA. Nucleic Acids Res., *29:* 3975–3981, 2001.
45. Jenner, T. J., deLara, C. M., O'Neill, P., and Stevens, D. L. Induction and rejoining of DNA double-strand breaks in V79-4 mammalian cells following γ-and α-irradiation. Int. J. Radiat. Biol., *64:* 265–273, 1993.
46. Lobrich, M., Cooper, P. K., and Rydberg, B. Non-random distribution of DNA double-strand breaks induced by particle irradiation. Int. J. Radiat. Biol., *70:* 493–503, 1996.
47. Zhou, R. H., Wang, P., Zou, Y., Jackson-Cook, C. K., and Povirk, L. F. A precise interchromosomal reciprocal exchange between hot spots for cleavable complex formation by topoisomerase II in amsacrine-treated Chinese hamster ovary cells. Cancer Res., *57:* 4699–4702, 1997.
48. Wang, P., Zhou, R. H., Zou, Y., Jackson-Cook, C. K., and Povirk, L. F. Highly conservative reciprocal translocations formed by apparent joining of exchanged DNA double-strand break ends. Proc. Natl. Acad. Sci. USA, *94:* 12018–12023, 1997.
49. Wang, P., Lee, J. W., Yu, Y., Turner, K., Zou, Y., Jackson-Cook, C. K., and Povirk, L. F. Gene rearrangements induced by the DNA double-strand cleaving agent neocarzinostatin: conservative non-homologous reciprocal exchanges in an otherwise stable genome. Nucleic Acids Res., *30:* 2639–2646, 2002.
50. Savage, J. R., and Simpson, P. J. FISH "painting" patterns resulting from complex exchanges. Mutat. Res., *312:* 51–60, 1994.